Supplementary Materials for

GDE2 promotes neurogenesis by glycosylphosphatidylinositol-anchor cleavage of RECK

Sungjin Park*, Changhee Lee*, Priyanka Sabharwal, Mei Zhang, Caren L. Freel Meyers and Shanthini Sockanathan**

* These authors contributed equally

** Author for correspondence:ssockan1@jhmi.edu

This PDF file includes:

Materials and Methods

Expression Constructs

GDE1 (NM_019580), GDE2 (NM_001037271), GDE3 (XM_420208), GDE6 (XM_417276), Dll1 (NM_007865), RECK (XM_418897), GPI-PLD (NM_008156), Notum (NM_175263) and Adam10 (NM_007399) expression constructs were cloned in the chick β-actin promoter vector (pCAGGS) unless otherwise specified. The GDE2.APML mutant was constructed by mutating the residues APML located within the GDPD domain to GAHD (*3*). In ovo electroporations were carried out as described (*1*, *2*). Sparse expression of GDE2, RECK-CD2, full-length and secreted forms of RECK in chick spinal cords was induced using a binary Cre-lox based expression system where coding sequences were preceded by loxP-STOP-loxP sites and coelectroporated with CMV-Cre expression plasmids at HH st12 (*3*, *24*). In these experiments a hyperactive form of GDE2 was used to gain efficient MN induction (GDE2C25S; *2*). A similar system was used for sequential RECK and GDE2 expression in HEK293T cells; however, CreER was used to obtain 4-hydroxy tamoxifen (4-OHT) inducibility of Cre activity and RECK coding sequences were flanked by two loxP sites and inserted upstream of the GDE2 coding sequence. Thus, RECK is expressed in the absence of 4-OHT, but 4-OHT incubation led to RECK excision and concomitant GDE2 expression.

In situ hybridization and immunofluorescent staining

In situ hybridization and immunostaining analyses were performed as previously described (*1*, *2*). Antibodies used: guinea pig-Olig2 (1:20,000; Ben Novitch); mouse anti-Isl2 (1:100; DSHB); goat anti-β-Gal (1:3000; Arnel); rat anti-BrdU (1:100; Sigma) Rabbit anti-Lbx1 (1:100; Martyn Goulding); rabbit anti-Brn3a (1:100; Abcam); rabbit anti-Engrailed (1:2000; Abcam); rabbit anti-Chx10 (1:2000; Thomas Jessell); Goat anti-Gata2/3 (1:100; SantaCruz). Detection of BrdU was carried out as described (*2*).

Chick *Hes5-1* and *Blbp* (FABP7) in situ probe sequences were respectively derived from the 3' region of the coding sequence and from the 3'UTR sequence based on NCBI reference sequence NM_001012695 and NM_205308 . RECK in situ probes were derived from ORF NCBI sequence XM_418897.

Cell-counts

Embryos were labeled with BrdU for 30 minutes after 24 hours to delineate the lateral extent of the VZ, dissected, embedded and sectioned (*2*). Counts of $Isl2^{+}$ cells in the ventricular zone of chick embryos were obtained from 10-20 sections/embryo (n=6-8 embryos). Construction of $Gde2^{-/-}$ animals and neuronal counts were performed as described (*3*).

ShRNA

Short hairpin (*sh*) RNAs were cloned into the pSilencer1.0-U6 vector (Ambion). *ShRNA* target sequences were as follows: 5' AATGGAATAAGCTGAGAGATT 3' for RECK *shRNA1*; 5'AACCAGAAATGTGGAAGGCAA 3' for RECK *shRNA2*; 5' AATTCGCGCCTAGGTCCGAAC 3 for control *shRNA*.

Cell-culture and Western blots

HEK293T cells were cultured in DMEM with 10% FBS on polyethyleneimine (PEI)-coated 12 well plates and transfected using Fugene6 agent (Roche). 24 hours after transfection, medium was changed to serum free DMEM and cells were incubated for an additional 24 hours. Medium and cell lysates were collected separately, and secretion and expression of proteins were analyzed by western blot and quantified using ImageJ (NIH). No differences in cell viability were found between cells transfected with RECK and GDE2, GDE2.APML or GDE1, suggesting that RECK detected in the medium is not a result of cell lysis. For Western analyses of chicken spinal cord lysate, chick spinal cords were electroporated at HH st12/13 and the spinal cords were harvested at HH st19/20. 10-12% SDS-PAGE in Tris-glycine buffer was used unless otherwise specified. Anitbodies used in Western analyses were rabbit-anti Jag1 (1:1000, Santa Cruz); rabbit-anti CRD (1:250, gift from Paul Englund); HRP-conjugated anti-Flag (1:5000, Sigma); rabbit-anti RECK (1:1000, Cell Signaling Technology); mouse-anti actin (1:3000, Sigma) and mouse anti-myc (1.5 μg/ml for IP, DSHB) and as described.

Triton X-114 partitioning

Triton X-114 (Sigma) partitioning of GPI-anchored proteins was performed as previously described with modifications (*17*). 2% Triton X-114 was pre-conditioned in 100 mM Tris-HCl, pH 7.4, 150 mM NaCl buffer.

Partitioning of secreted proteins in medium: Culture medium was incubated with TritonX-114 buffer (final 1%) and was maintained on ice for 10 min with occasional mixing. Two phases were separated by raising the temperature to 30^0C for 5 min, followed by centrifugation (3000 x g, 3 min, RT). The detergent-rich pellet was collected for membrane-bound proteins. Detergent-poor supernatant was subject to repeated separation steps and collected.

Extraction and partitioning of total protein from cells: Cells were washed with PBS twice and were incubated with 1% Triton X-114 buffer for 10 min at 4^0C. Resuspended cells were incubated on ice for 10 min with occasional mixing and were centrifuged at 16,000 x g for 15 min at 4^0C. Supernatants were separated as described in partitioning of medium.

Extraction and partitioning of brain lysate: E12.5 cortices of *Gde2*$^{-/-}$ animals and WT littermates were dissected and sonicated in 1% Trion X-114 buffer. The lysates were incubated for 30 min on ice with occasional vortexing and centrifuged at 16,000 x g for 15 min at 4^0C. Supernatants were partitioned as described above.

Radiolabeling of cells

One day after transfection of HEK293T cells, cells were labeled overnight with 20 μCi/ml of [^{3}H] ethanolamine (Moravek Biochmicals), 0.1 mCi/ml of [^{3}H] myo-inositol (PerkinElmer), or 0.1 mCi/ml [^{32}P] Pi (PerkinElmer) in serum free DMEM. For inositol labeling, inositol-free DMEM was used (MP biomedicals). The medium was immunoprecipitated (IPed) with a myc antibody for 3 hours, followed by a 1 hour incubation with GammaBind G Sepharose (GE Healthcare). IP complexes were washed 4 times with PBST (1% Triton X-100). Radioactivity incorporated in IPed samples was measured using a liquid-scintillation counter and normalized to the amount of RECK IP detected by Western blot.

In vitro glycerophophodiester phosphodiesterase (GDPD) assay

HEK293T cells were transiently transfected with GDE1 or GDE2. Two days later, post nuclear membrane fractions were prepared (*27*) and used in enzyme assays. Preparation of substrates and implementation of the enzyme-coupled spectrophotometric assay were as previously described (*13*) with modifications. 15μg of membrane proteins were incubated with 0.5 mM substrate in 100 mM Tris buffer (pH 7.5, 10 mM $MgCl_2$ or 5 mM $CaCl_2$) at 30^{o}C for 30 min. The reaction was stopped by adding perchloric acid (final 0.5 N). After neutralization with potassium carbonate solution, the amount of glycerol-3-phosphate (G3P) was measured by the absorbance change at 340 nm in hydrazine buffer (0.2 M hydrazine, 0.5 M Glycine, pH 9.5, 2.87 mM EDTA, 2.5 mM NAD, 0.1 mg/ml of G3P dehydrogenase). G3P level was normalized to GDE1 level after subtracting background level without enzyme.

Chemical synthesis

Cyclic G[1,2] phosphate synthesis was performed using the protocol described (*28*).

Surface biotinylation assay

Surface biotinylation assay was performed as previously described (*29*). Briefly, thirty hours after transfection of HEK293T cells with RECK/GDE and CreER constructs, cells were cooled on ice, washed twice with ice cold PBS++ (1X PBS, 1 mM $CaCl_2$, 0.5 mM $MgCl_2$) and then incubated with PBS++ containing 1 mg/ml Sulfo-NHS-SSBiotin (Pierce) for 30 min at 4 °C. Unreacted biotin was quenched by PBS++ containing 100 mM Glycine. Cultures were harvested in RIPA buffer, sonicated, and centrifuged at 132,000 rpm for 20 min at 4 °C. The supernatant was rotated with Streptavidin beads (Pierce) for 2 hr at 4 °C. Precipitates were washed with RIPA buffer three times and eluted with SDS gel loading buffer.

For the live biotinylation assay, thirty hours after transfection of HEK293T cells with RECK/vector, RECK/GDE or RECK/GPI-PLD constructs, cells were cooled on ice, washed twice with ice cold PBS++ (1X PBS, 1 mM $CaCl_2$, 0.5 mM $MgCl_2$) and then incubated with PBS++ containing 1 mg/ml Sulfo-NHS-SSBiotin for 10 min on ice. Unreacted biotin was quenched by cold serum-containing medium (10% FBS). Cells were then incubated in serum-free medium for additional 4 hours. Biotinylated proteins from the lysate and medium were precipitated with Streptavidin beads.

FACS and data analyses

Chick spinal cords were electroporated with Dll1-IRES-EGFP together with empty, GDE2 or ADAM10 expression constructs at HH st12/13 and harvested at HH st19/20. Dissected spinal cords were incubated in Accumax (Sigma) for 15min at room temperature and dissociated by pipetting. Dissociated cells were labeled with Phyco-Erythrin (PE)-conjugated Dll1 ECD antibody (LSBio, 1:150 dilution) and washed twice with 1X HBSS. Mouse spinal cords from E9.5 *HB9:GFP; Gde2*$^{+/+}$ and *HB9:GFP; Gde2*$^{-/-}$ embryos were dissected, dissociated and labeled as above.

Fluorescence intensity of PE and GFP in individual cells were recorded by FACS Calibur Analytic Flow Cytometer (BD) according to the manufacturer's instructions. For each sample, data from 10,000-50,000 live cells were collected and analyzed with standard R package flowCore and flowViz from Bioconductor (*30-33*). Cells from mouse

spinal cords typically fell into 3 groups according to GFP expression level (GFP-negative, GFP-low, GFP-high), reflecting previous reports that GFP expression in HB9-GFP animals is robust in MNs but weaker in a subset of ventral interneurons (*34*). GFP-high populations were analyzed for each embryo to maximize analysis of Dll1 expression in MNs, and this group was obtained by fitting the GFP signal distribution to a gaussian mixture model. The median value of PE signals (representing Dll1 expression levels) in the GFP-high group was calculated and compared. In the case of chick spinal cords, GFP^+ cells were selected by setting a threshold based on non-electroporated samples to remove auto-fluorescent cells. The PE signal was normalized to the GFP signal to control for electroporation efficiency prior to analysis.

Statistcal Analysis

All statistical tests utilized unpaired two-tailed Student's t-test.

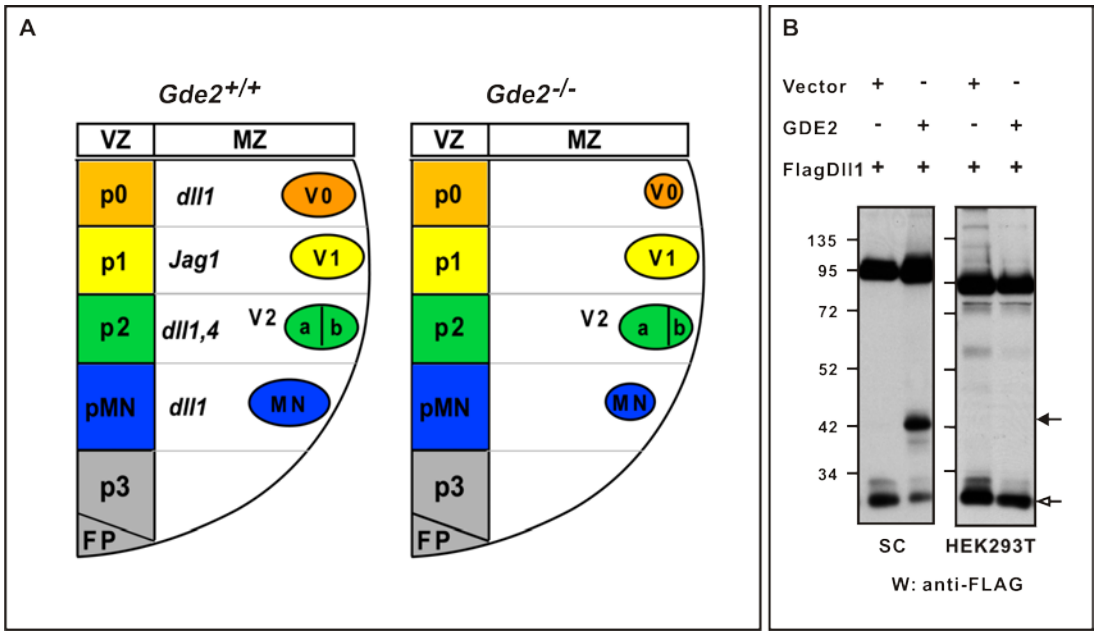

Figure S1. GDE2 targets Dll1 function

(A) Schematic of the ventral spinal cord summarizing *Gde2*$^{-/-}$ phenotypes that coincide with domains of Dll1 expression and function. VZ=ventricular zone; MZ=marginal zone; FP=floorplate. P=progenitor. Although decreased numbers of the MN and V0 interneurons in *Gde2*$^{-/-}$ animals are consistent with increased Notch signaling, the V2 interneuron phenotype resembles Notch inactivation (*35*); these collective observations imply that GDE2 can either activate or inhibit Notch signaling according to cellular context. (B) Western blots of electroporated spinal cord extracts (SC) and transfected HEK293T cells showing that GDE2 can induce Dll1-42 (black arrow) in electroporated spinal cords but not in transfected HEK293T cells. Open arrow shows a processed 30kD Dll1 C-terminal fragment.

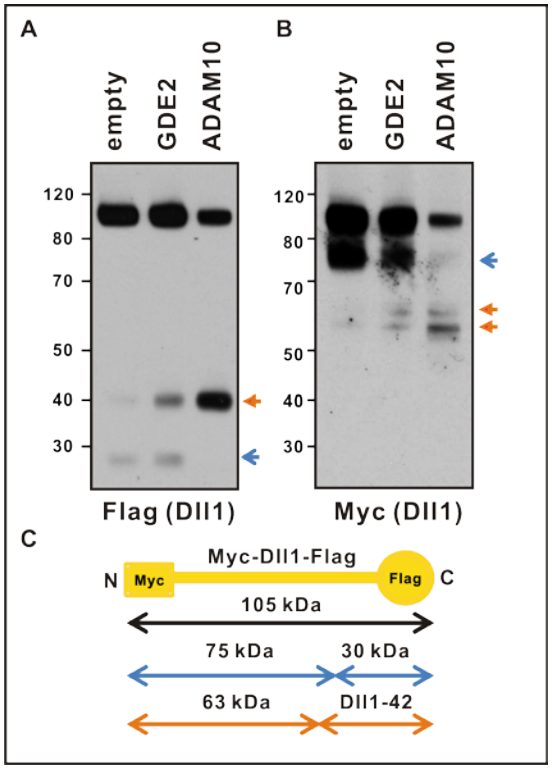

Figure S2. Processing of Dll1 by GDE2 and ADAM10

(A, B) Processing of N-terminal Myc and C-terminal Flag double-tagged Dll1 (Myc-Dll1-Flag) in extracts prepared from chick spinal cords electroporated with GDE2 or ADAM10 was analyzed by 4-12% gradient SDS-PAGE in MES buffer. Control electroporations generated full length Dll1 (105kD), an approximately 30kD C-terminal form (blue arrow, A, C), very low levels of Dll1-42 (orange arrow, A, C) and a 75kD N-terminal fragment (blue arrow, B, C). GDE2 coelectroporated with Myc-Dll1-Flag resulted in the same fragments as control, but generated robust levels of a C-terminal 42kD Dll1 product (Dll1-42) (orange arrow, A, C) and concomitantly higher levels of N-terminal tagged 63kD and 60kD Dll1 ECDs (orange arrows, B, C). We attribute the presence of two N-terminal tagged Dll1 ECDs to increased processing and/or degradation in vivo. Electroporation with ADAM10 generated the same Dll1 products with the exception of the 30kD fragment in (A). The absence of the 30kD fragment may be due to ADAM10 preferentially cleaving at the 42kD site in vivo. Alternatively, the 30kD product may be formed by ADAM10- independent proteases as described previously (*10*).

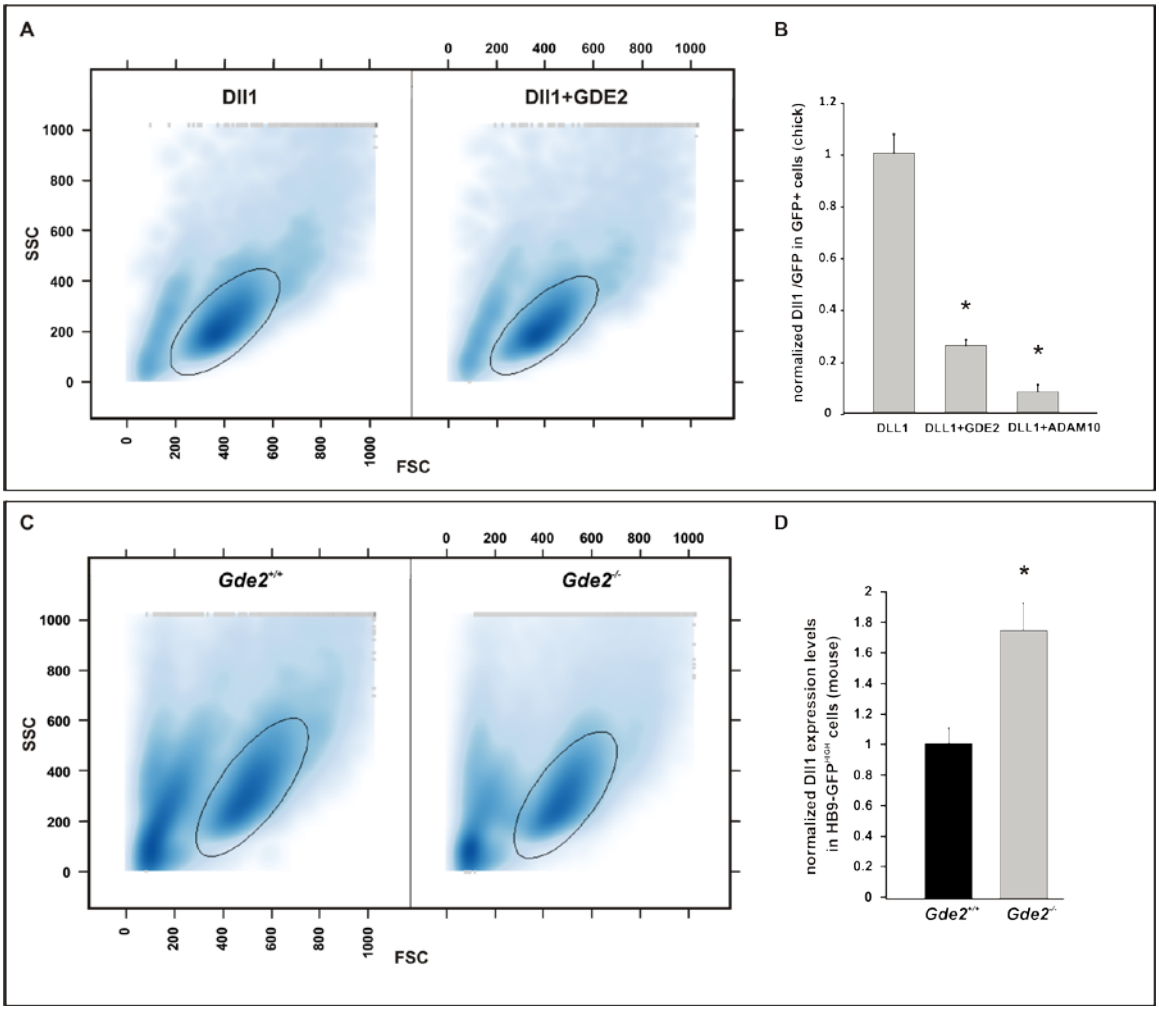

Figure S3. GDE2 activity alters surface expression of Dll1 in vivo.

(A, C) Graphs showing all sorted cells for dissociated chick (A) and mouse (C) spinal cords separated according to Forward Scatter (FSC) and Side Scatter (SSC) levels. The distribution profiles of FSC and SSC among embryos in both cases were comparable. The elipse represents gated live cells that were analyzed for Dll1 surface expression.
(B) Graph quantifying Dll1 surface expression in chick spinal cord cells electroporated with Dll1-IRES-GFP using FACS analysis (see Methods). Dll1 surface expression (normalized by electroporation efficiency) per cell is markedly reduced in cells coexpressing either GDE2 or ADAM10. Mean $\pm$ s.e.m., n=4-5 embryos. Dll1 vs Dll1+GDE2 p=0.005; Dll1 vs Dll1+ADAM10 p=0.0017; two-tailed t-test. (D) Graph quantifying Dll1 surface expression in mouse MNs labeled by GFP (HB9-GFP^{HIGH}) using FACS. Median Dll1 surface expression of HB9-GFP^{HIGH} cells is significantly higher in *Gde2*$^{-/-}$ E9.5 embryos compared with *Gde2*$^{+/+}$ controls. Mean $\pm$ s.e.m., n=8-10 embryos; p=0.00527, two-tailed t-test.

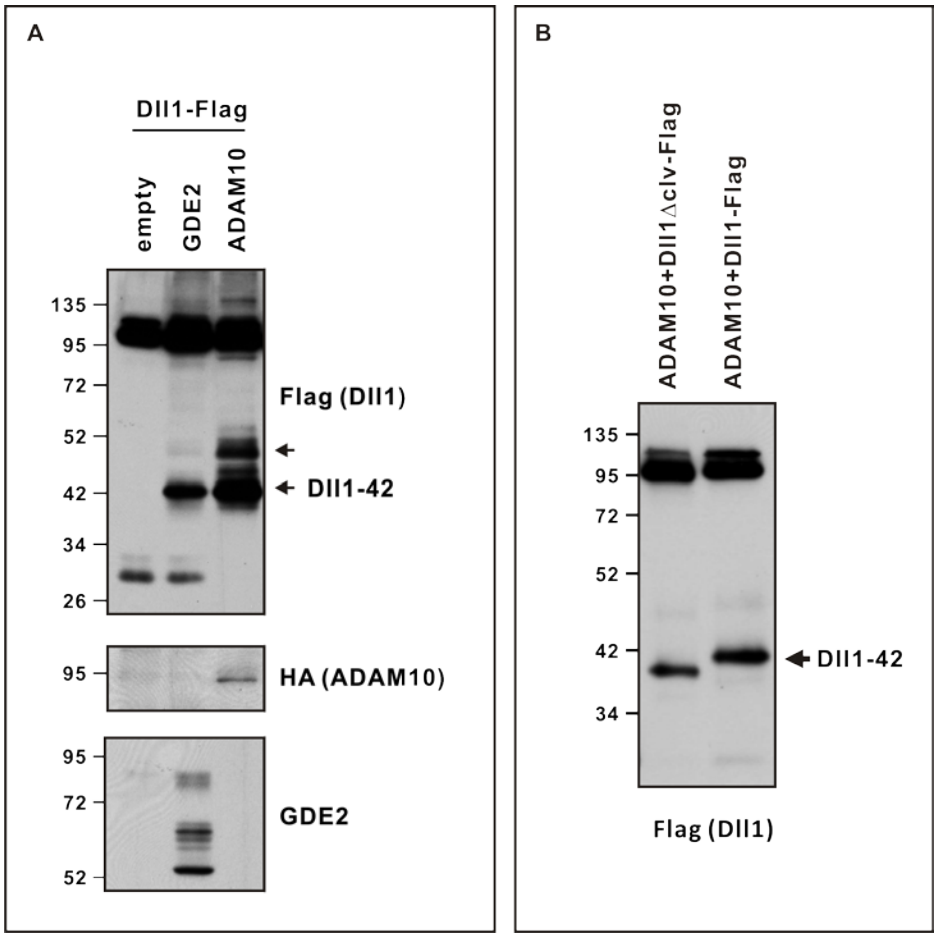

Figure S4. ADAM10 induces Dll1-42 in electroporated spinal cords.

(A, B) Western blots of protein extracts prepared from chick spinal cords electroporated with constructs expressing C-terminal tagged Dll1-Flag, Dll1Δclv-Flag and vector alone (empty), GDE2 or ADAM10. ADAM10 and Dll1 co-expression generates robust levels of Dll1-42 but not the 30kD form of Dll1. On rare occasions a 50kD form is generated (arrow) and might reflect degradation of full-length Dll1, utilization of additional ADAM10 cleavage sites or posttranslational modification of Dll1-42. (B) ADAM10 retains the ability to cleave Dll1Δclv, a form of Dll1 lacking an ADAM10 cleavage site mapped in vitro (*10*). This observation suggests that Dll1-42 is generated through a novel ADAM10 cleavage site upstream of Δclv. Nevertheless, ADAM10 expression generates Dll1-42 as does GDE2 (arrow), supporting the model that ADAM activity lies downstream of GDE2.

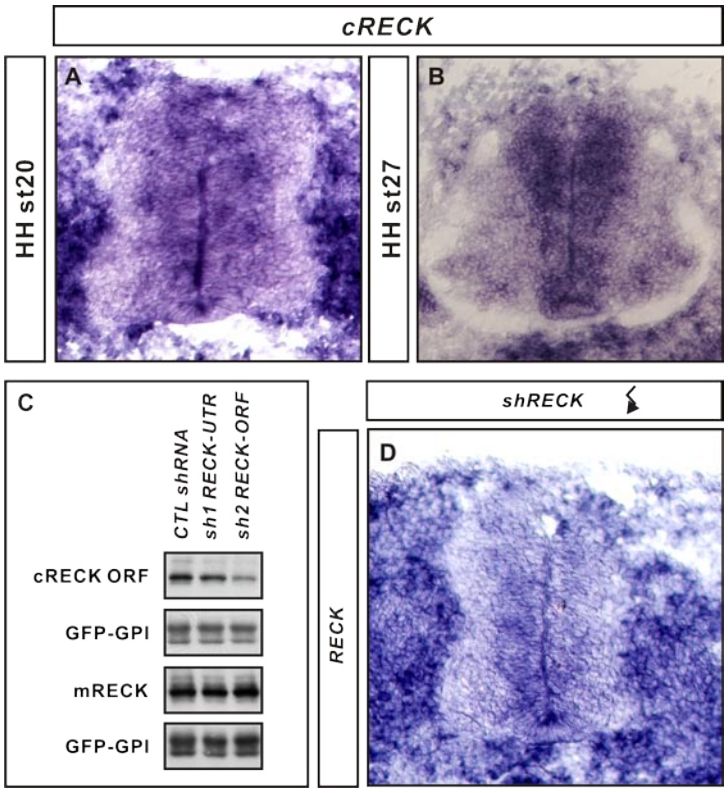

Figure S5. RECK expression and knockdown by *shRNA*.

(A, B, D) Coronal sections of WT (A, B) and electroporated (D) chick spinal cords showing in situ hybridization of *RECK* transcripts. At HH st20 *RECK* mRNAs are detected in the ventricular zone (VZ) and in the intermediate zone (IZ) where GDE2 resides; however, by HH st27, *RECK* expression is enriched in VZ cells. (C) Western blots of transfected HEK293T cells showing that *shRNA1* directed against the chick *RECK* 3'UTR does not cause knockdown of RECK expressed from plasmids expressing the RECK ORF alone, whereas *shRNA2* directed against the *RECK* ORF does; in both cases no knockdown of mouse RECK or GPI-anchored GFP is detected. No knockdown is observed on transfection of control *shRNAs*. (D) Electroporation of *shRNA* in chick spinal cords shows ablation of *RECK* expression. Right side is electroporated.

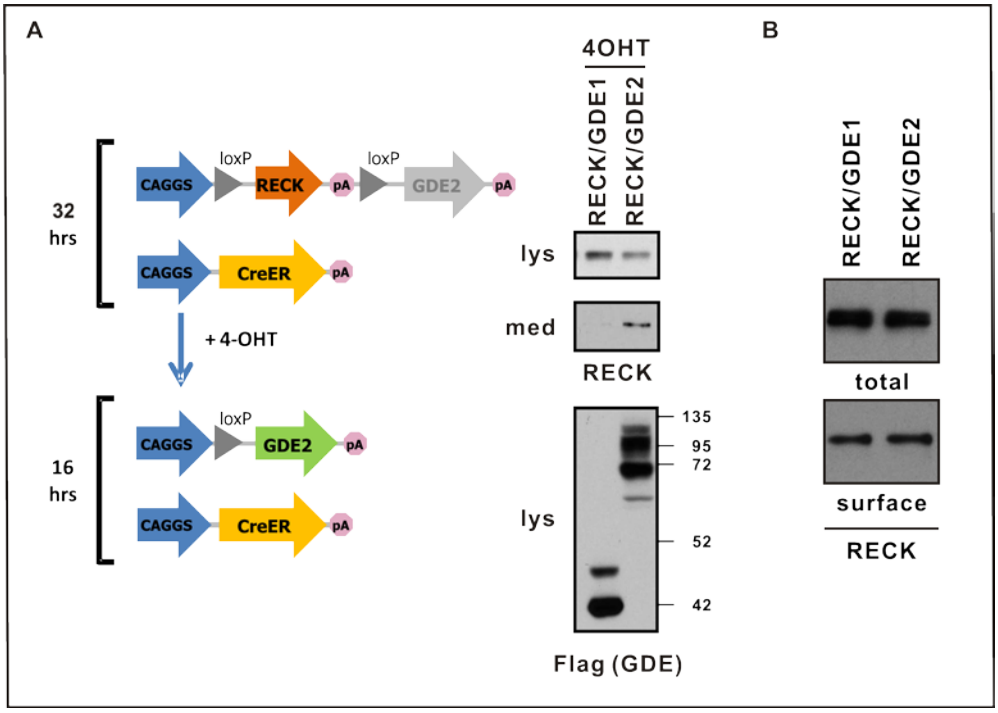

Figure S6. Sequential expression of RECK and GDE2 leads to RECK release to the medium

(A) Schematic showing RECK induction (32 hours) followed by RECK silencing and GDE2 expression upon 4-OHT addition (16 hours). This strategy maximizes the production of mature GPI-anchored RECK on the surface and should minimize immature forms of RECK in the secretory system. Western blots show that sequential expression of RECK and GDE2 led to RECK release to the medium, whereas the same experiment with RECK and GDE1 did not. (B) RECK is localized to the cell surface after 32 hours. Western blot of total and surface biotinylated RECK 32 hours after transfection in HEK293T cells, confirming surface localization of RECK prior to 4-OHT induced Cre-mediated excision of RECK and induction of GDE2.

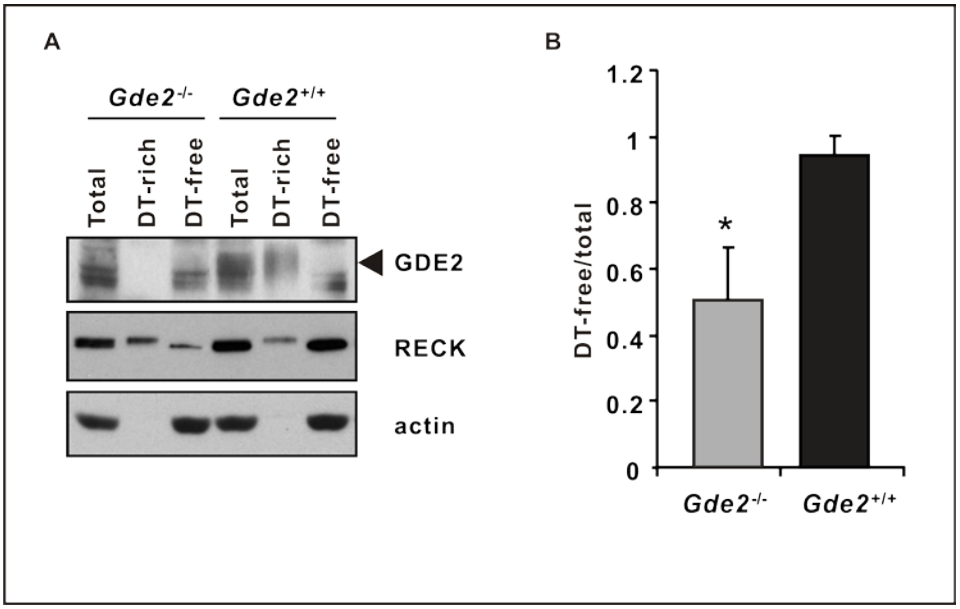

Figure S7. Loss of GDE2 leads to decreased levels of cleaved RECK in vivo.

(A) Representative Western blot of cortical extracts prepared from E12.5 cortices of *Gde2*$^{-/-}$ animals and WT littermates. Triton X-114 extraction shows a significant reduction of RECK in the detergent (DT) free phase compared with WT littermates. (B) Densitometry analysis of quantifying levels of RECK in DT-free fractions of WT and *Gde2*$^{-/-}$ littermates in relation to total RECK protein. Two-tailed t-test, mean $\pm$ s.e.m. *p=0.04, n= 4.

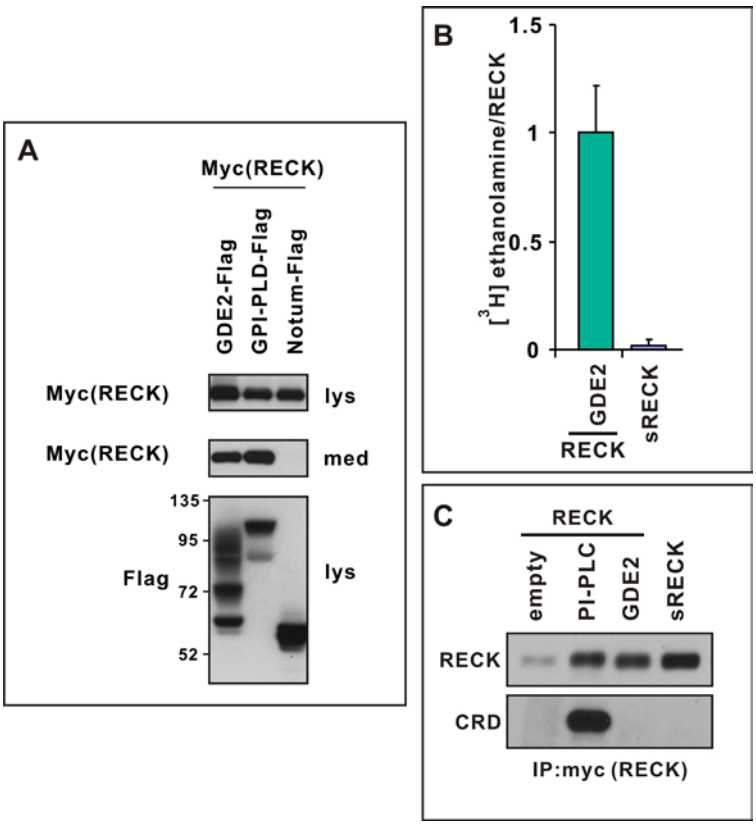

Figure S8. Characterization of GPI-anchor cleavage of RECK.

(A) Western blot of lysates (lys) and medium (med) of HEK293T cells transfected with Myc-tagged RECK and C-terminal Flag tagged GDE2, GPI-PLD or Notum. GDE2 and GPI-PLD release RECK into the medium but not Notum, suggesting that Notum is unable to cleave RECK. (B) Graph quantifying amount of radiolabelled ethanolamine incorporated into RECK expressed with GDE2 or secreted (s) RECK. Mean $\pm$ s.e.m. n=4-12. (C) Western blots of IPs of RECK from transfected HEK293T cells shows reactivity with CRD antibodies only after treatment with PI-PLC.

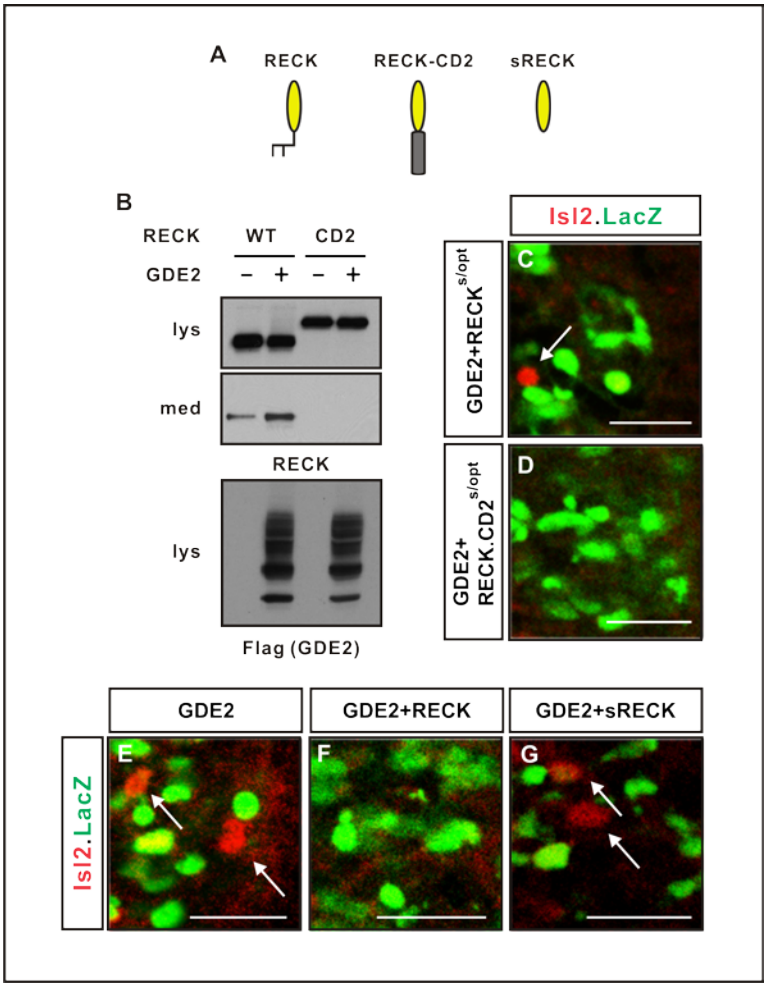

Figure S9. Manipulation of membrane-tethered RECK alters RECK function.

(A) Schematic of WT RECK with GPI-anchor, RECK-CD2 (CD2 transmembrane domain replaces the GPI-anchor), sRECK (lacks GPI-anchor). (B) Western blots of lysates (lys) and medium (med) of HEK293T cells transfected with GDE2 and WT RECK or RECK-CD2, showing that in contrast to WT GPI-anchored RECK, GDE2 fails to cleave RECK-CD2 and release the RECK ECD into the medium. (C, D) Representative images of sectioned electroporated chick spinal cords showing that suboptimal levels of plasmids expressing $RECK^{s/opt}$ results in moderate suppression of non cell-autonomous GDE2-dependent MN differentiation (arrow) while similar amounts of $RECK\text{-}CD2^{s/opt}$ abolishes premature MN generation by GDE2. (E-G) Representative images of sectioned chick spinal cords showing that electroporation of plasmids expressing sRECK fails to suppress GDE2-dependent induction of MN differentiation (red cells, arrows), while GPI-anchored RECK effectively suppresses GDE2 function. All $GDE2^{+}$ cells express RECK (data not shown). Scale bar = 20μm.

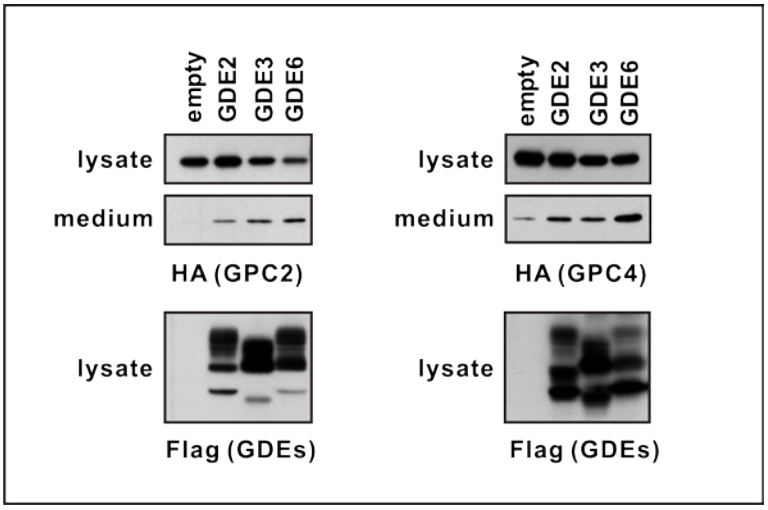

Figure S10. Six-transmembrane GDPD proteins release GPI-anchored proteins from the membrane.

Western blots of protein extracts of transfected HEK293T cells showing that all members of the six transmembrane GDE family, ie. GDE2, GDE3 and GDE6 can release the ECDs of GPI-anchored glypican 4 (GPC4) and GPI-anchored glypican 2 (GPC2) into the medium.

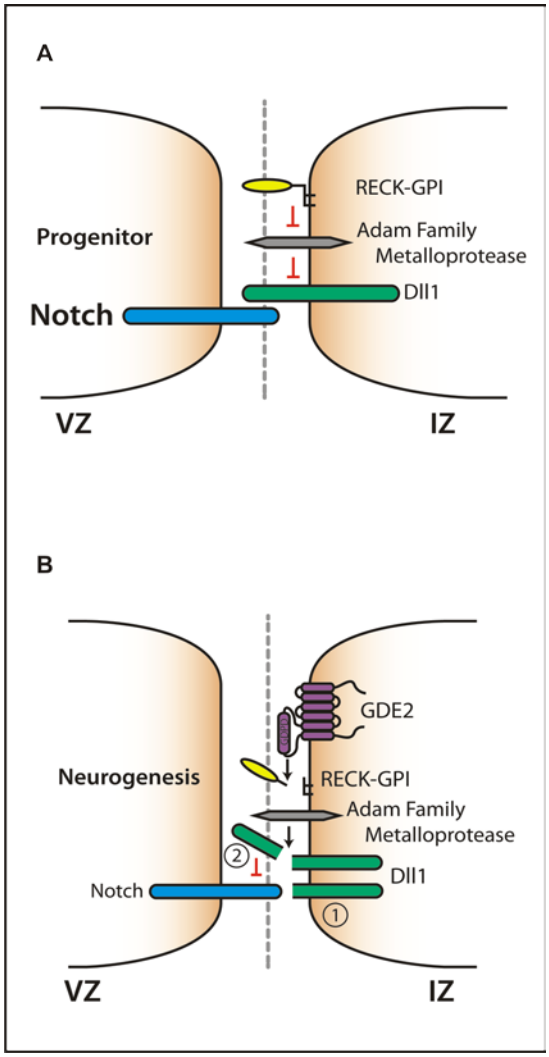

Figure S11. Model of GDE2 function in the developing spinal cord.

(A) RECK in IZ cells prevents ADAM cleavage of Dll1 enabling Dll1/Notch binding, Notch activation in adjacent progenitors and VZ progenitor maintenance. (B) GDE2 in newly differentiating MNs in the IZ cleaves RECK in cis, enabling ADAM metalloproteases to cleave Dll1. Dll1 ECD is generated (2), active Dll1 is cleared from the membrane (1), which together downregulate Notch signaling in adjacent progenitors to initiate MN differentiation.

	[^{32}P]Pi/RECK	p-value	[^{3}H]inositol/RECK	p-value	[^{32}P]Pi/[^{3}H]inositol	p-value
GDE2	1.00 ± 0.26	0.0035	1.00 ± 0.37	0.26	0.88 ± 0.16	0.0015
GPI-PLD	0.47 ± 0.09		0.77 ± 0.11		0.52 ± 0.04	

Table S1. GDE2 does not induce PLD cleavage

HEK 293T cells were transfected with RECK/GDE2 or RECK/GPI-PLD and fed with [^{32}P] Pi and [^{3}H] inositol in serum-free and inositol-free medium for 40 hours. RECK released into the medium was immunoprecipitated and the amount of radiolabel incorporated and RECK protein were measured by scintillation counting and western blot analysis respectively. n=8 (GDE2); n=4 (GPI-PLD).

Supplementary References

27. P. Lin *et al*., The mammalian calcium-binding protein, nucleobindin (CALNUC), is a Golgi resident protein. *J. Cell Biol*. **141**, 1515-1527 (1998).
28. L. Kugel, M. Halmann, Hydrolysis of glycero-1, 2-cyclic phosphate. *J. American Chem. Soc*. **89**, 4125-4128 (1967).

29. J. H. Hu *et al.*, Homeostatic scaling requires group I mGluR activation mediated by Homer1a. *Neuron* **68**, 1128-1142 (2010).

30. R Development Core Team, R: A Language and Environment for Statistical Computing. R Foundation for Statistical Computing Vienna, Austria ISBN 3-900051-07-0 (2010).

31. R.C. Gentleman *et al*., Bioconductor: Open software development for computational biology and bioinformatics. *Genome Biology* **5**, R80 (2004).

32. B. Ellis, P. Haaland, F. Hahne, N.L. Meur, N. Gopalakrishnan, FlowCore: Basic structures for flow cytometry data. R package version 1.16.0.

33. B. Ellis, R. Gentleman, F. Hahne, N.L. Meur, D. Sarkar, FlowViz: Visualization for flow cytometry. R package version 1.14.0.

34. H. Wichterle, I. Lieberam, J.A. Porter, T.M. Jessell, Directed differentiation of embryonic stem cells into MNs. *Cell* **110**, 385-397 (2002).

35. C. Y. Peng *et al*., Notch and MAML signaling drives Scl-dependent interneuron diversity in the spinal cord. *Neuron* **53**, 813-827 (2007).